Electronic Supplementary Information

Pt Cocatalyst Morphology on Semiconductor Nanorod Photocatalysts Enhances Charge Trapping and Water Reduction

Bumjin Park,‡[a] Won-Woo Park,‡[b] Ji Yong Choi,‡[a] Woong Choi,[a] Young Mo Sung,[c] Soohwan Sul,*[c] Oh-Hoon Kwon *[b] and Hyunjoon Song *[a]

[a] Department of Chemistry, Korea Advanced Institute of Science and Technology, Daejeon 34141, Republic of Korea

[b] Department of Chemistry, Ulsan National Institute of Science and Technology, Ulsan 44919, Republic of Korea

[c] Analytical Engineering Group, Samsung Advanced Institute of Technology, Samsung Electronics Co., Ltd., Suwon 16678, Republic of Korea

‡These authors contributed equally to this work.

EXPERIMENTAL SECTION

Materials. Cadmium oxide (CdO, 99.99+%), trioctylphosphine oxide (TOPO, 99%), trioctylphosphine (TOP, 90%), selenium (Se, 99.99%), platinum(II) acetylacetonate [$Pt(acac)_2$, 97%], 1,2-dichlorobenzene (anhydrous, 99%), 1,2-hexadecanediol (90%), diphenyl ether (99%), hexadecylamine (98%), 1-adamantanecarboxylic acid (99%), oleylamine (70%), oleic acid (90%), 11-mercaptoundecanoic acid (MUA, 95%), tetramethylammonium hydroxide pentahydrate (>97%), sodium sulfide nonahydrate (>98%), and sodium sulfite (≥98%) were purchased from Sigma-Aldrich. 1-Tetradecylphosphonic acid (TDPA, 98%) was purchased from Alfa Aesar. Other solvents were purchased from Junsei.

Synthesis of bare CdSe nanorods. CdO (0.062 g, 0.48 mmol), TDPA (0.55 g, 2.0 mmol), and TOPO (3.5 g, 9.1 mmol) were put into the 25 mL double neck flask and degassed under vacuum for 30 min. The mixture was elevated to 320 ℃ and stirred for 20 min under a nitrogen atmosphere. The Se-TOP (0.05 M, 4.0 mL) solution of Se (0.014 g, 0.18 mmol) in TOP was added to the reaction mixture, and the reaction temperature was lowered to 270 ℃. The resulting mixture was stirred for 10 min. The color of the mixture changed to brown during the reaction. After cooling down the mixture, the product was precipitated by adding 2-propanol, followed by centrifugation at 10000 rpm. The final product was dispersed in toluene.

Synthesis of Pt-CdSe nanorods with round tips (Round). 1,2-Hexadecanediol (0.022 g, 0.085 mmol), oleylamine (0.10 mL, 0.31 mmol), oleic acid (0.10 mL, 0.32 mmol), and diphenyl ether (5.0 mL, 32 mmol) were mixed into the flask and placed under vacuum at 80 ℃ for 30 min. In another flask, $Pt(acac)_2$ (0.033 g, 0.084 mmol) was mixed with the CdSe nanorod dispersion in dichlorobenzene (9.0 mg, 5.0 mL), and the mixture was stirred under a nitrogen atmosphere at 65 ℃ for 10 min. The resulting nanorod dispersion was injected into the former

flask, and the mixture was stirred at 225 ℃ for 5 min. The reaction was quenched using a water bath, and the product was precipitated by adding 2-propanol and centrifuging at 5000 rpm. The final product was dispersed in toluene.

Synthesis of Pt-CdSe nanorods with cubic tips (Cubic). 1,2-Hexadecanediol (0.022 g, 0.085 mmol), oleylamine (0.10 mL, 0.31 mmol), oleic acid (0.10 mL, 0.32 mmol), and diphenyl ether (5.0 mL, 32 mmol) were mixed into the flask and placed under vacuum at 80 ℃ for 10 min. After degassing, the mixture was bubbled with CO gas for 20 min. In another flask, $Pt(acac)_2$ (0.030 g, 0.076 mmol) was mixed with the CdSe nanorod dispersion in dichlorobenzene (9.0 mg, 5.0 mL), and the mixture was stirred under a nitrogen atmosphere at 65 ℃ for 10 min. The resulting nanorod dispersion was injected into the former flask, and the mixture was stirred at 200 ℃ for 15 min. The reaction was quenched using a water bath, and the product was precipitated by adding 2-propanol and centrifuged at 5000 rpm. The final product was dispersed in toluene.

Synthesis of Pt-CdSe nanorods with rough tips (Rough). 1,2-Hexadecanediol (0.11 g, 0.43 mmol), hexadecylamine (0.37 g, 1.5 mmol), 1-adamantanecarboxylic acid (0.025 g, 0.14 mmol), and diphenyl ether (5.0 mL, 32 mmol) were put into the flask and degassed under vacuum at 60 ℃. The flask was charged with nitrogen, and the reaction temperature was elevated to 120 ℃. In another flask, $Pt(acac)_2$ (0.026 g, 0.066 mmol) was mixed with the CdSe nanorod dispersion in dichlorobenzene (9.0 mg, 5.0 mL), and the mixture was stirred under a nitrogen atmosphere at 65 ℃ for 10 min. The resulting nanorod dispersion was injected into the former flask, and the mixture was stirred at 215 ℃ for 5 min. The reaction was quenched using a water bath, and the product was precipitated by adding 2-propanol and centrifuging at 5000 rpm. The final product was dispersed in toluene.

Characterization. The Pt-CdSe nanorods were characterized by transmission electron microscopy (TEM, Philips Tecnai F20 operated at 200 kV, KAIST) and high-resolution TEM (HRTEM, FEI Tecnai G2 F30 S-Twin operated at 300 kV, KAIST). X-ray diffraction (XRD) patterns were recorded using a Rigaku SmartLab at KAIST. UV-visible absorption spectra were measured by a Shimadzu UV-3600 spectrophotometer with a 1 cm quartz cuvette in toluene. The photoluminescence spectra were collected using a spectrophotometer (QM-400, Photon Technology International) using a 1 cm quartz cuvette. The atomic ratio of the catalysts was estimated using iCAP 6300 Duo inductively coupled plasma-atomic emission spectroscopy (ICP-AES).

Phase transfer to the aqueous phase. 11-Mercaptoundecanoic acid (0.050 g, 0.23 mmol) was mixed in methanol (5.0 mL), and tetramethylammonium hydroxide pentahydrate was added into the solution to fix the pH at 11. The nanorods were dispersed in the solution, and the mixture was stirred for 30 min. The final products were precipitated by adding toluene and centrifuging at 10000 rpm. Finally, the nanorods were dispersed in deionized water.

Photocatalytic hydrogen-evolution reaction study. The catalyst dispersion in an aqueous solution (10 mL) was placed into the 36 mL quartz flask. The catalyst amount was 1.5 mg based on the elemental analysis using ICP-AES. 0.35 M Na_2SO_3/0.25 M Na_2S aqueous solution (10 mL) was added to the flask and sealed with a rubber septum. Before the photocatalytic reaction, the mixture was bubbled with nitrogen gas for 15 min. The reaction was performed using the Xe lamp (300 W, Oriel) as light source with the UV cut-off and liquid optical filters. The gas inside the reactor was periodically collected using a syringe. The amount of hydrogen was quantitatively analyzed using gas chromatography (YL6100, Youngin) with a thermal conductivity detector (TCD).

Calculation of quantum yields. The quantum yield (QY) for hydrogen generation was calculated by using the following equation according to the literature:[S1]

$$\mathrm{QY}(\%) = \frac{n_e}{n_p} \times 100 = \frac{2n_{H_2}}{n_p} \times 100$$

where n_e is the number of electrons participating in the hydrogen-evolution reaction, n_p is the number of photons absorbed by the light source, and n_{H_2} is the number of generated hydrogen molecules. The light source for measuring QY was a light-emitting diode (M420L3 Violet, Thorlabs) emitting at 420 nm (13 mW).

Photoelectrochemical measurements. To prepare the working electrode, a fluorine-doped tin oxide (FTO) glass was washed with acetone and methanol for 30 min and dried for 1 h. The catalysts with the mixture of hexane (0.10 mL) were loaded onto the electrode. The catalyst amount used for each electrode was fixed at 0.5 mg. Then, 30 μL of a diluted Nafion solution (50 μL of Nafion perfluorinated resin solution in 0.95 mL of 2-propanol) was loaded onto the electrode. The photoelectrochemical characterization was carried out using a three-electrode system consisting of the working electrode, a Pt wire counter electrode, and a Ag/AgCl reference electrode. The working electrode area exposed to the electrolyte was 0.50 cm^2. A 300 W Xe lamp with the UV cut-off was used as a light source and measured to be 100 mW cm^{-2}. The photocurrent responses were recorded using a BioLogic SP-150 potentiostat. The electrochemical impedance spectroscopy (EIS) was measured to depict Nyquist plots. The EIS was obtained using BioLogic SP-150 potentiostat and scanned from 200 kHz to 100 mHz under visible light irradiation.

Transient-absorption (TA) spectroscopy. TA measurements were performed using the pump-probe method. Detailed experimental procedure of TA measurements has been reported elsewhere.[S1] For the femtosecond-resolved TA measurement, we used an amplified ytterbium-

based laser system (Pharos, Light Conversion), which produces IR pulses (6 W, 200 kHz) centered at 1030 nm with the pulse width of ~170 fs. We reduced the repetition rate to 1 kHz by using a pulse picker to fully relax carriers/excitons before successive pulsed excitation. The pump beam of 550 nm was generated using an optical parametric amplifier (Orpheus, Light Conversion). We used a sapphire crystal to generate white light pulses by using the IR pulses. To avoid anisotropic effects, the polarization of the pump pulse was set at 54.7° (magic angle) with regard to the polarization of the probe pulse. To avoid multi-excitonic dynamics, the pump fluence was reduced to 5.3 μJ/cm^2 (**Fig. S8**). Pump and probe pulses were focused and overlapped on the sample plane. The transmitting white-light probe pulses were directed into a photodiode array (Kymera, Andor).

Nanosecond-resolved TA measurements were performed using a TA spectrometer (EOS, Ultrafast Systems) coupled to a Ti:Sapphire regenerative amplifier (Libra, Coherent) and an optical parametric amplifier (TOPAS, Light Conversion). A part of the output of the amplifier (pulse duration = 50 fs; repetition rate = 1 kHz; center wavelength = 800 nm) was used to pump the optical parametric amplifier that delivered pump pulses at 550 nm for the TA measurements. We used Nd:YAG laser (STM, Luekos) to produce sub-nanosecond white-light probe pulses by pumping optical fiber. The time delays between the pump and probe pulses were regulated by electrically synchronizing the Nd:YAG laser and the Ti:Sapphire regenerative amplifier. All spectroscopic measurements were carried out at an ambient temperature. Obtained TA transients were fitted to multi-exponential functions convoluted with the Gaussian-shape instrument response functions (IRF) using a data analysis software (Igor, WaveMetrics). Global-lifetime analyses of TA spectra were performed using a software (CarpetView, Light Conversion).

Electrochemical active surface area (ECSA) measurement for metal tips. An indium tin oxide (ITO) glass was washed with acetone and methanol for 10 min and dried for 10 min in air. According to the literature,[S2] the nanorod samples were treated at 185 ℃ in an air furnace for 5 h to remove the surfactant by low-temperature thermal annealing. The mixture of chloroform (0.10 mL) with each sample (0.50 mg) was loaded dropwise on the ITO glass. The underpotential deposition (UPD) of Cu was carried out on a nitrogen-saturated 0.05 M H_2SO_4/0.05 M $CuSO_4$ solution. The cyclic voltammetry (CV) was conducted on a potentiostat at a scanning rate of 5 mV s^{-1}.[S3]

Derivation of equation (1) for photocatalytic hydrogen evolution.

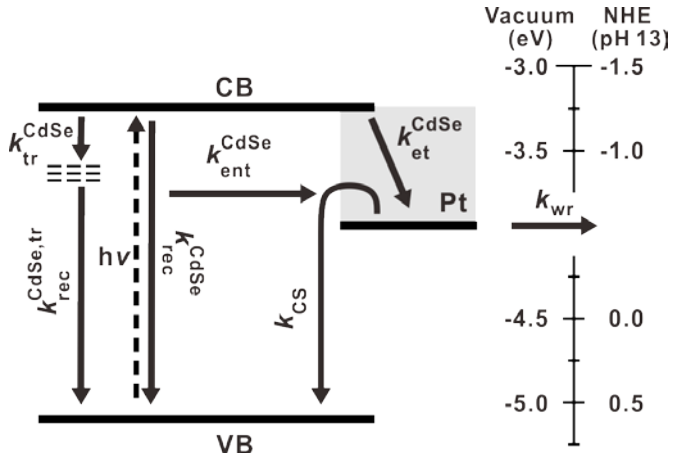

In this kinetic model, the CS state is described as a continuum considering the metallic nature of Pt. Then, the rate equation for each state is given by the model carrier pathway:[S1]

$$d[CB]/dt = -k_{rec}^{CdSe}[CB] - k_{tr}^{CdSe}[CB] - k_{et}^{CdSe}[CB] - k_{ent}^{CdSe}[CB],$$

$$d[Pt]/dt = k_{et}^{CdSe}[CB] - k_{CS}[Pt] - k_{wr}[Pt],$$

$$d[H_2]/dt = k_{wr}[Pt]$$

Then, the hydrogen evolution rate can be integrated as follows:

$$[H_2] = [CB]_0 \times k_{wr} \times \left[\left\{ \frac{k_{et}^{CdSe}}{(k_{tr}^{CdSe} + k_{rec}^{CdSe} + k_{et}^{CdSe} + k_{ent}^{CdSe} - k_{CS} - k_{wr})} \times \frac{1}{k_{tr}^{CdSe} + k_{rec}^{CdSe} + k_{et}^{CdSe} + k_{ent}^{CdSe}} \right\} \right.$$

$$\times e^{-(k_{tr}^{CdSe} + k_{rec}^{CdSe} + k_{et}^{CdSe} + k_{ent}^{CdSe})t} - \left\{ \frac{k_{et}^{CdSe}}{(k_{tr}^{CdSe} + k_{rec}^{CdSe} + k_{et}^{CdSe} + k_{ent}^{CdSe} - k_{CS} - k_{wr}) \times (k_{CS} + k_{wr})} \right\}$$

$$\left. \times e^{-(k_{CS} + k_{wr})t} \right]$$

$$+ C \qquad \text{(S1)}$$

The boundary condition is at $t = 0$, $[H_2] = 0$:

$$C = -[CB]_0 \times k_{wr} \times \left\{ \frac{k_{et}^{CdSe}}{(k_{tr}^{CdSe} + k_{rec}^{CdSe} + k_{et}^{CdSe} + k_{ent}^{CdSe} - k_{CS} - k_{wr})} \times \frac{1}{k_{tr}^{CdSe} + k_{rec}^{CdSe} + k_{et}^{CdSe} + k_{ent}^{CdSe}} - \frac{k_{et}^{CdSe}}{(k_{tr}^{CdSe} + k_{rec}^{CdSe} + k_{et}^{CdSe} + k_{ent}^{CdSe} - k_{CS} - k_{wr}) \times (k_{CS} + k_{wr})} \right\} \quad \text{(S2)}$$

thus

$$C = [CB]_0 \times k_{wr} \times \frac{k_{et}^{CdSe}}{k_{tr}^{CdSe} + k_{rec}^{CdSe} + k_{et}^{CdSe} + k_{ent}^{CdSe} - k_{CS} - k_{wr}} \left\{ - \frac{1}{k_{tr}^{CdSe} + k_{rec}^{CdSe} + k_{et}^{CdSe} + k_{ent}^{CdSe}} + \frac{1}{(k_{CS} + k_{wr})} \right\} \quad \text{(S3)}$$

According to the previous works, we can assume the following condition:[S1,S4]

$$k_{CS} + k_{wr} \ll k_{tr}^{CdSe} + k_{rec}^{CdSe} + k_{et}^{CdSe} + k_{ent}^{CdSe}$$

Then, we simplify equation S2 as:

$$C = [CB]_0 \times k_{wr} \times \frac{k_{et}^{CdSe}}{k_{tr}^{CdSe} + k_{rec}^{CdSe} + k_{et}^{CdSe} + k_{ent}^{CdSe}} \times \frac{1}{(k_{CS} + k_{wr})} \quad \text{(S4)}$$

$$\text{At } t = \infty,\ [H_2] = C = [CB]_0 \times \frac{k_{et}^{CdSe}}{k_{tr}^{CdSe} + k_{rec}^{CdSe} + k_{et}^{CdSe} + k_{ent}^{CdSe}} \times k_{wr} \times \left(\frac{1}{k_{CS} + k_{wr}} \right) \quad \text{(S5)}$$

Because $[CB]_0 \propto A_{CdSe}$, thus,

$$[H_2] \propto A_{CdSe} \times \frac{k_{et}^{CdSe}}{k_{tr}^{CdSe} + k_{rec}^{CdSe} + k_{et}^{CdSe} + k_{ent}^{CdSe}} \times \frac{k_{wr}}{(k_{CS} + k_{wr})}$$

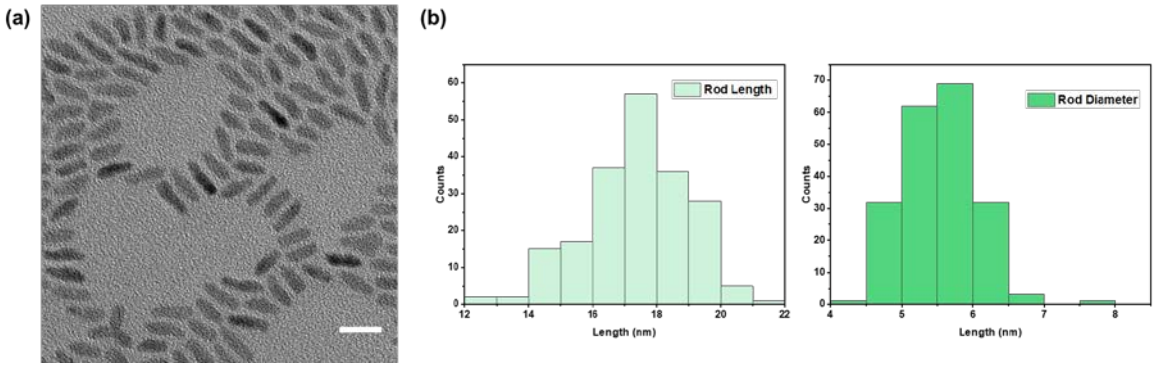

Fig. S1 (a) TEM image of bare CdSe nanorods. The bar represents 20 nm. (b) Histograms of the length and diameter of the bare CdSe nanorods. The average length and diameter were 17.4 ± 1.6 and 5.6 ± 0.5 nm, respectively.

Table S1. Elemental analysis data of Pt-CdSe nanorods measured by ICP-AES.

	Cd (%)	**Se (%)**	**Pt (%)**
Round	29.6	29.2	41.2
Cubic	32.0	27.8	40.2
Rough	33.8	31.9	34.3

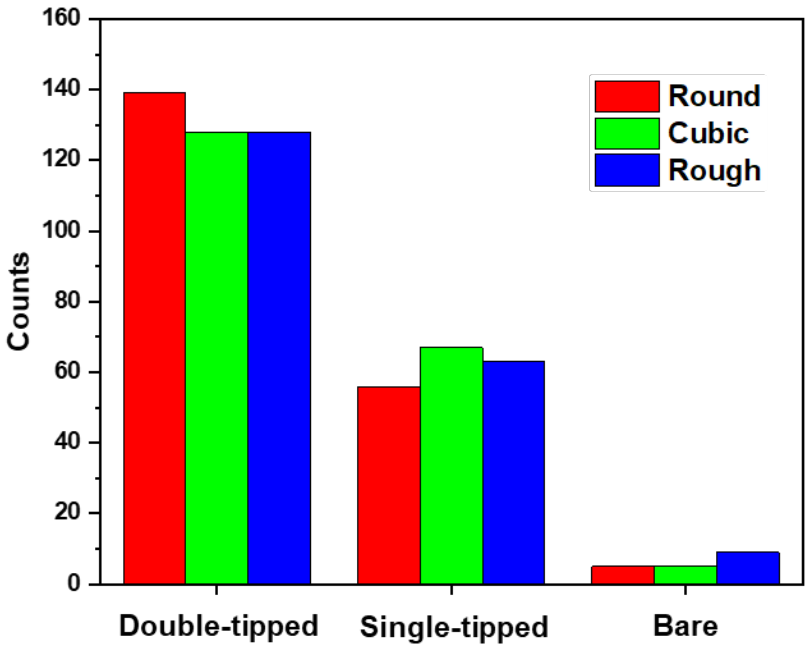

Fig. S2 Structural distributions of double-tipped, single-tipped, and bare nanorods for **Round**, **Cubic**, and **Rough**.

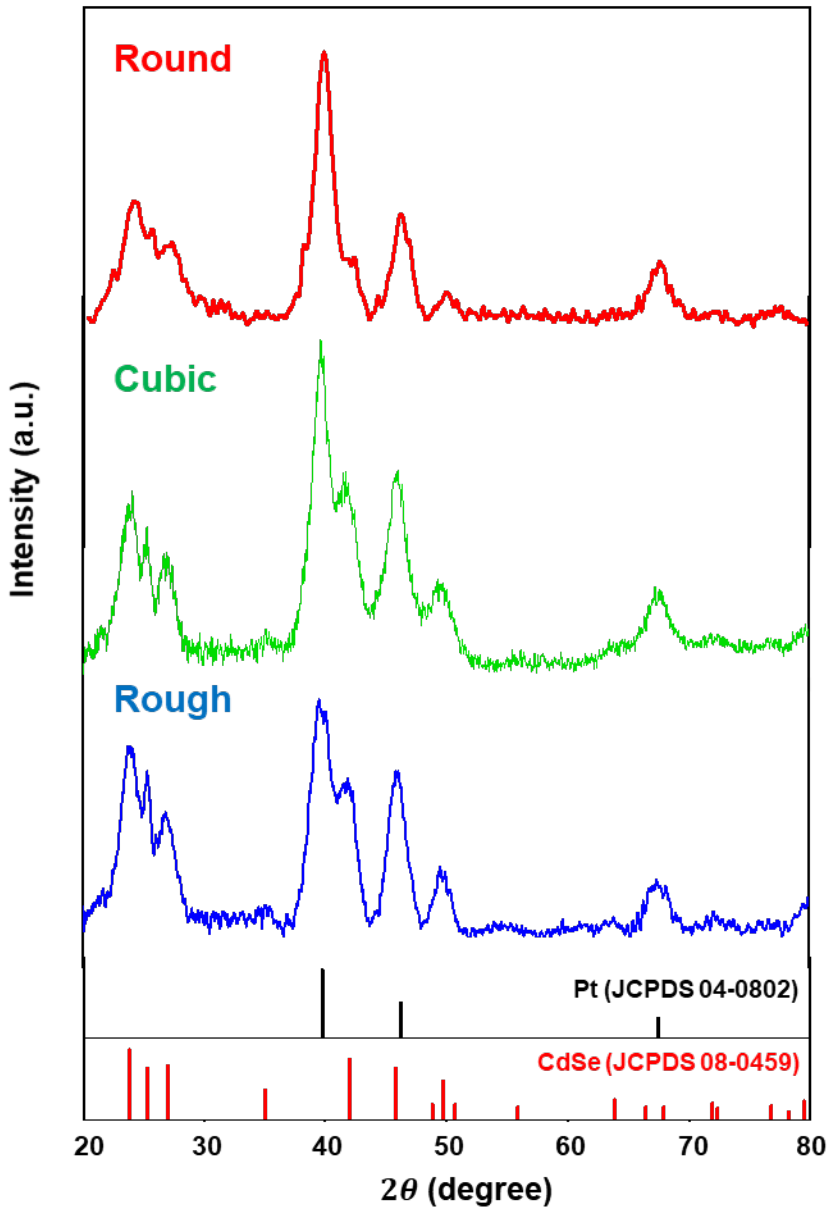

Fig. S3 X-ray diffraction (XRD) patterns of **Round**, **Cubic**, and **Rough**.

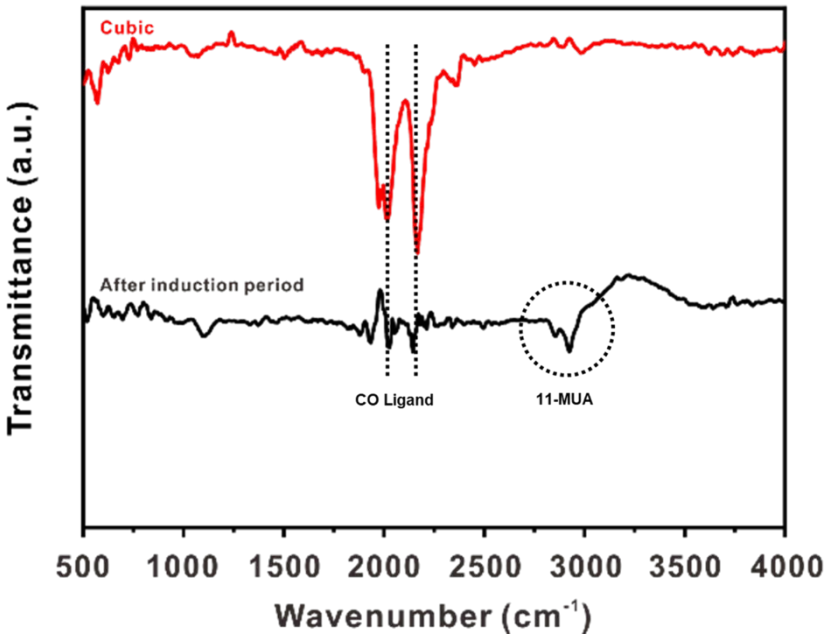

Fig. S4 FTIR spectra of **Cubic** as-synthesized and after the induction period.

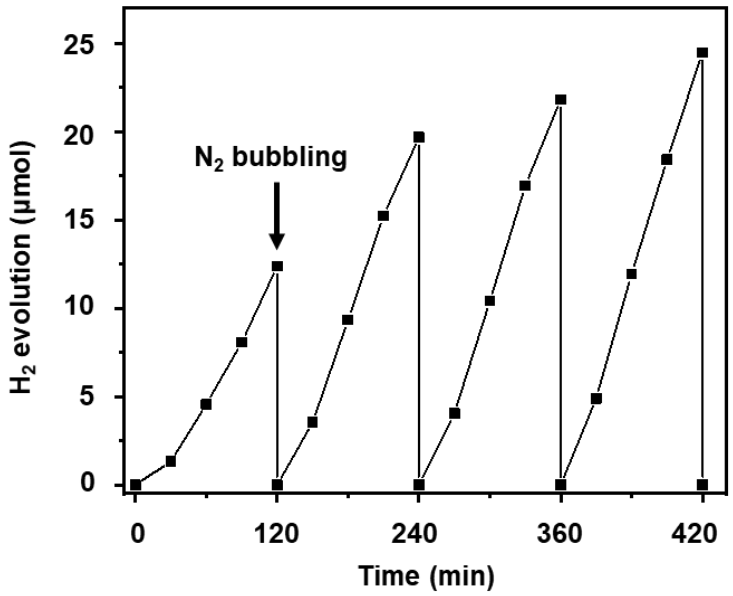

Fig. S5 Photocatalytic stability tests of **Rough**. The reaction was carried out with four cycles of a 2 h-reaction after N_2 purging.

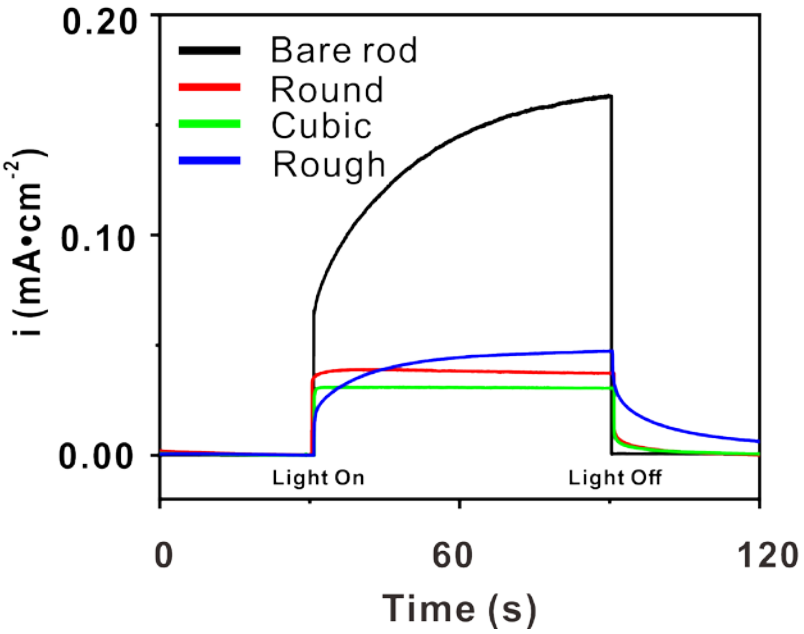

Fig. S6 Current-time photoresponse curves of bare rod (black), **Round** (red), **Cubic** (green), and **Rough** (blue) in a 0.35 M Na_2SO_3/0.25 M Na_2S aqueous solution.

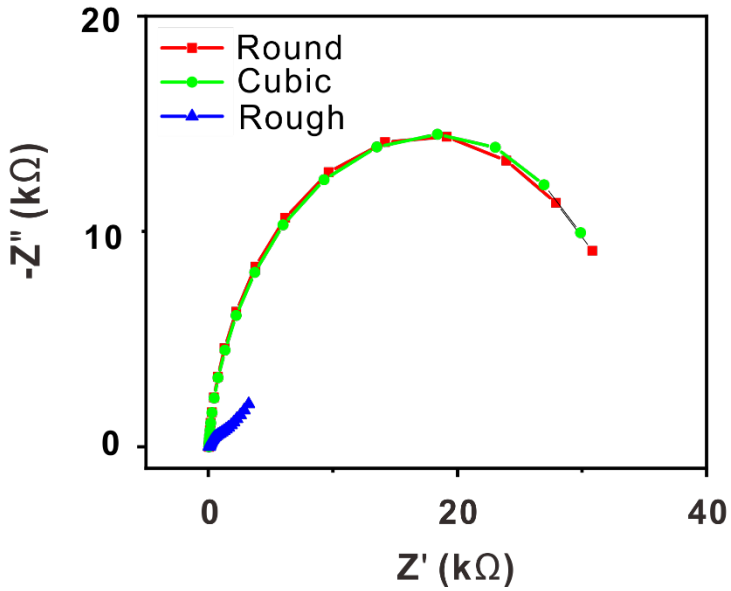

Fig. S7 Nyquist plots of **Round** (red), **Cubic** (green), and **Rough** (blue) in 0.35 M Na_2SO_3/0.25 M Na_2S aqueous solution under irradiation ($\lambda \geq 420$ nm).

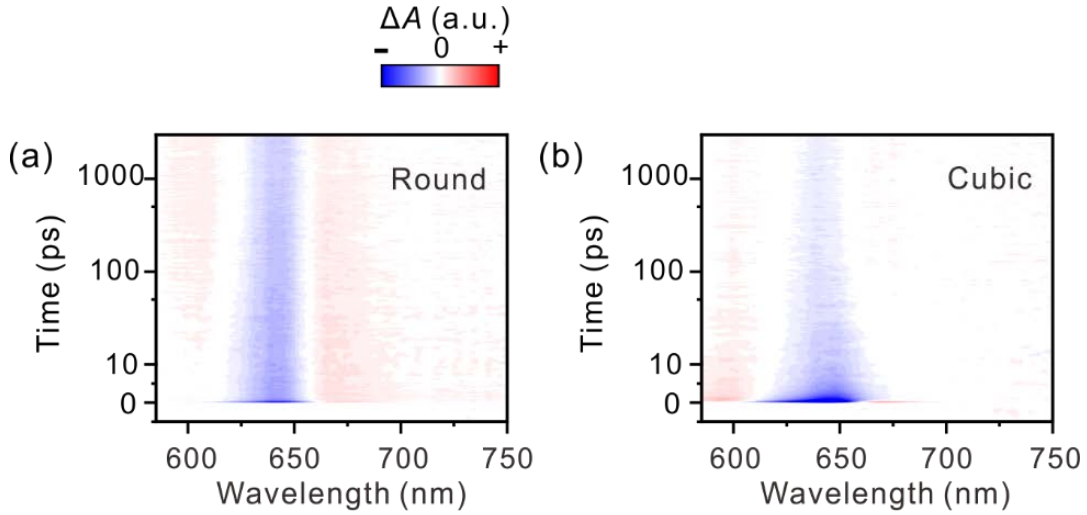

Fig. S8 Femtosecond-resolved TA spectroscopy. TA maps of CdSe nanorods with (a) **Round** and (b) **Cubic**. All TA maps were obtained with the excitation at 550 nm under the single-excitonic condition.

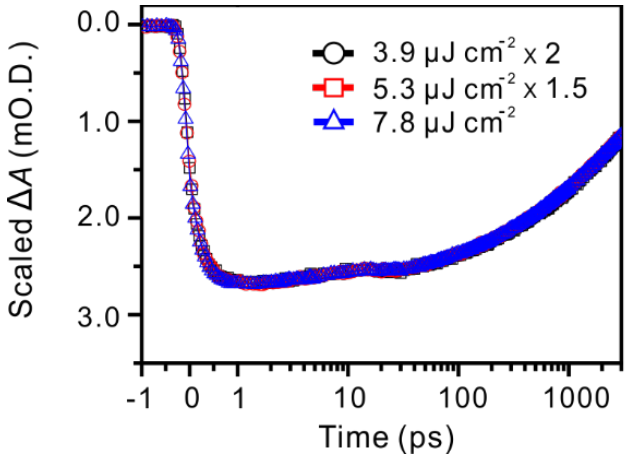

Fig. S9 Fluence dependence of the carrier dynamics. Femtosecond-resolved bleach-recovery kinetic profiles of bare CdSe rods monitored at 648 nm with different excitation fluences. The transients showed identical dynamics regardless of the fluence at least up to 7.8 μJ/cm^2. The pump fluence was set at 5.3 μJ/cm^2 for all samples to ensure single-excitonic dynamics.

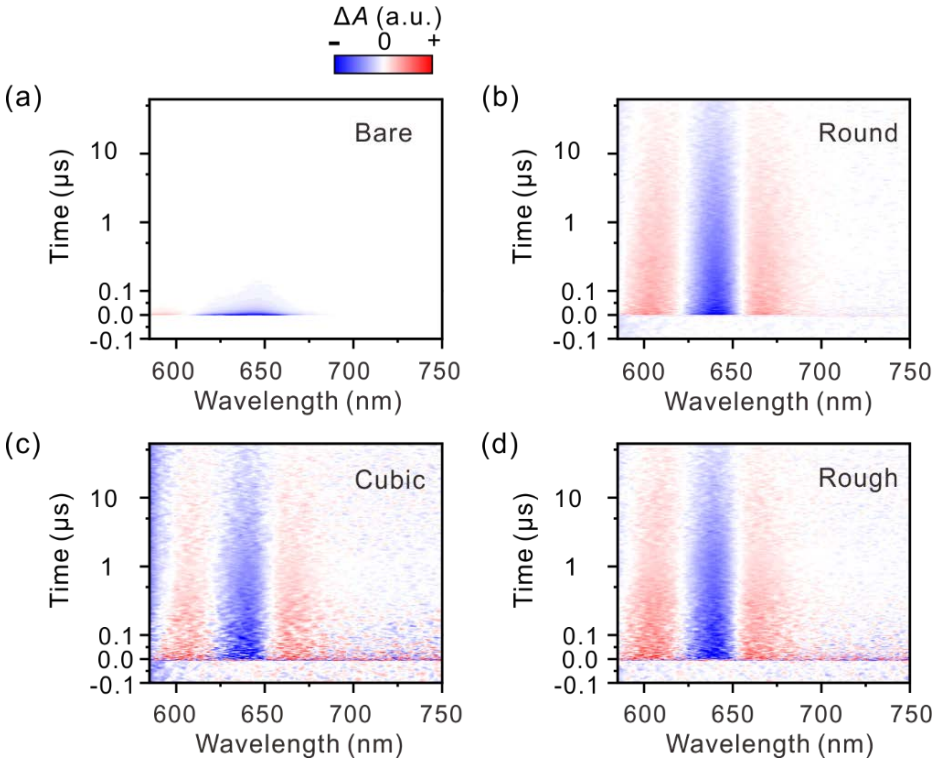

Fig. S10 Nanosecond-resolved TA spectroscopy. TA maps of (a) bare rods, (b) **Round**, (c) **Cubic**, and (d) **Rough**. All TA maps were obtained with the excitation at 550 nm. The excitons of the bare rod were fully depleted within sub-microsecond. The TA spectra of all Pt-CdSe nanorods persisted on a microsecond timescale and showed a symmetric, peak-dip-peak spectral feature.

Global-lifetime analysis.

Global-lifetime analysis was performed to investigate the evolution of the charge-separated (CS) state. Global-lifetime analysis on TA spectra across wavelength and time helps distinguish multiple absorbing species and reveal their kinetic entanglement.[S5] For satisfactory analysis, at least four lifetime components were introduced for both the bare and metal-tipped rods.

1. Bare CdSe rods

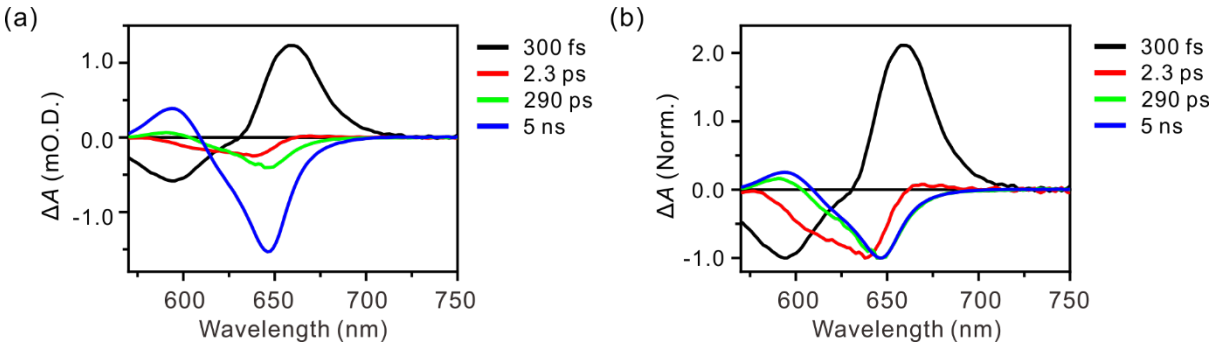

Fig. S11 Global-lifetime analysis of bare CdSe rods. (a) Lifetime-associated spectra according to the global-lifetime analysis on the femtosecond-resolved TA spectra of bare CdSe rods. (b) Normalized lifetime-associated spectra for comparison of the spectral shapes. Global lifetimes are given next to the left panel.

The exciton in the bare rod mainly relaxes on a timescale of several nanoseconds (**Table S2**). The lifetime-associated spectra of the 290-ps and 5-ns components show almost identical spectral features indicating that at least two relaxation pathways exist for the exciton (**Fig. S11b**). A previous study has reported that there exist multiple relaxation pathways for excitons/carriers in CdSe quantum dots, including emissive carrier-trapped states.[S6] The heterogeneity comprising size, shape, and surface-trap site leads to various relaxation pathways.

The fastest component represents the formation of the 290-ps and the 5-ns components in 300 fs. The spectral feature and the timescale of the fastest component match those of the intra-band relaxation of hot carriers to the band edge.[S7] It has been reported that surface trapping of a carrier in the CdSe quantum dot occurred on a few picosecond timescales.[S8, S9] Carrier trapping reduces the carrier population at the band edge. Thus, the spectral feature of the 2.3-ps component may arise due to the state-filling process from the upper excited state to the band edge following the carrier-trapping dynamics in CdSe.

2. Metal-tipped nanorods (Round, Cubic, and Rough)

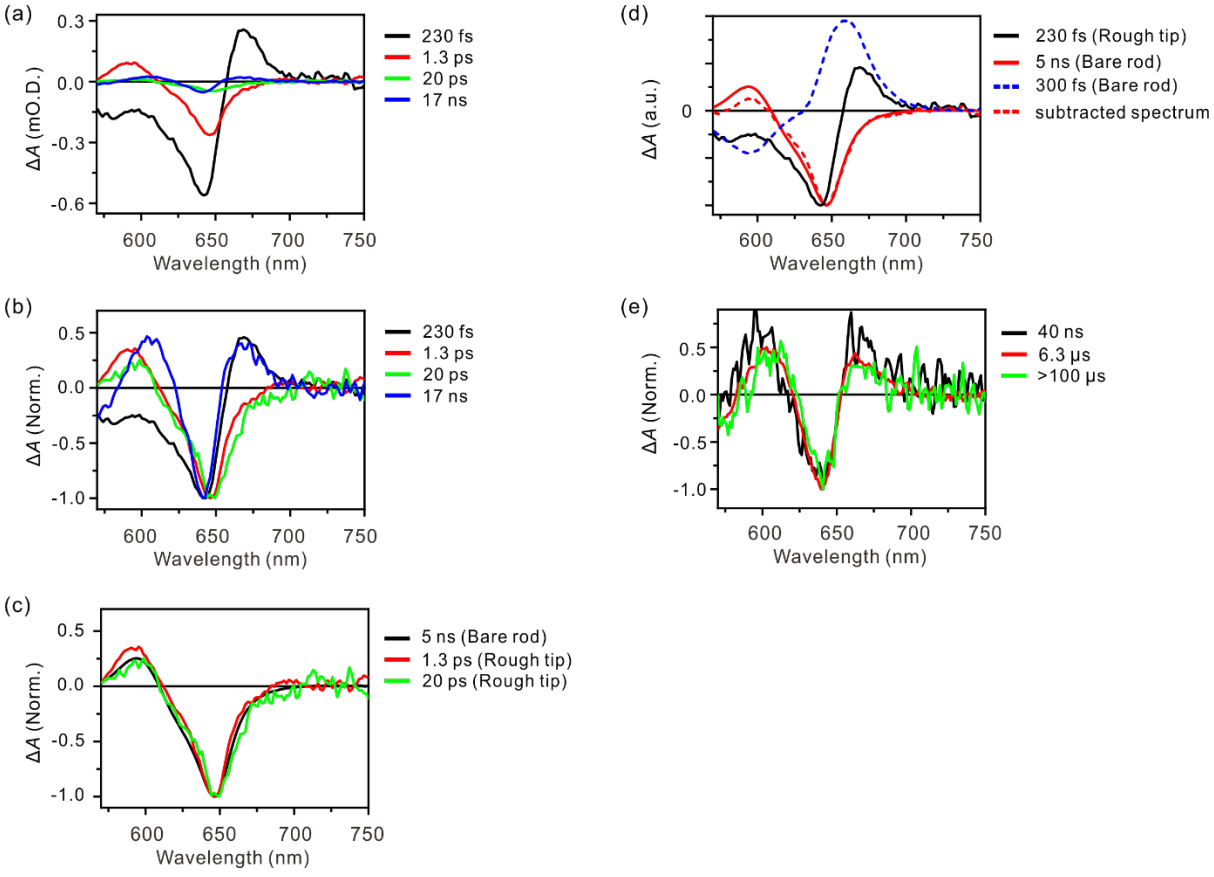

Fig. S12 Global-lifetime analysis of nanorods with rough tips. (a) Lifetime-associated spectra according to the global-lifetime analysis on the femtosecond-resolved TA spectra of **Rough**. (b) Normalized lifetime-associated spectra for comparison of the spectral shapes. (c)

Normalized lifetime-associated spectra of the 5-ns component of bare rods and the 1.3-ps (red) and 20-ps (green) components of **Rough**. The 5-ns component of the bare rod corresponds to the exciton relaxation within the rod. (d) Spectral deconvolution of the 230-fs (black) component of **Rough**. (e) Normalized lifetime-associated spectra according to the global-lifetime analysis of nanosecond-resolved TA. Global lifetimes are given next to each panel.

The lifetime-associated spectra of **Rough**, obtained by the global-lifetime analysis of the femtosecond-resolved TA measurements, show four-lifetime components: 230 fs, 1.3 ps, 20 ps, and 17 ns (**Fig. S12a and b**). The spectral features of the 1.3-ps and 20-ps components are identical to that of the 5-ns component of the bare rod (**Fig. S12c**). The timescale of the fastest component (230 fs) in **Rough** is similar to that of the intra-band relaxation in the bare rod (**Fig. S11a**). When the lifetimes of different absorbing species are similar, the lifetime-associate spectra often lead to misinterpretation of spectral features to transient species. By subtracting the scaled spectrum corresponding to the intra-band relaxation (300-fs component in **Fig. S11a**) from the apparent lifetime-associated spectrum of the 230-fs component, the processed spectrum matches those of the excitons relaxing in the bare rod, *i.e.*, the 5-ns component of the bare rod (**Fig. S12d**).

In contrast, the spectral feature of the weak 17-ns component is unique compared to the lifetime-associated spectra for the bare rod. We infer that a new transient species developed due to the presence of the Pt tips, *i.e.*, a CS state. A similar spectral feature has been reported for CdSe–MV^{2+} complexes and CdSe–Pt heterostructures.[S10] Both MV^{2+} and Pt were attributed to electron quenchers for CdSe. It follows that the symmetric, peak-dip-peak-shape spectra originate from remaining carriers at the CS state in the CdSe domain, *i.e.*, holes. Accordingly, unique peak-dip-peak spectral features of the nanosecond-resolved lifetime-associated spectra

indicate that the dynamics occurring on the nanosecond to microsecond timescale in the hybrid systems correspond to the relaxation of the CS state (**Fig. S12e**).

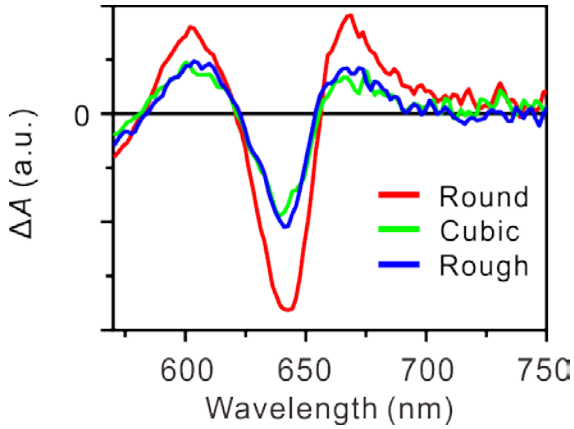

Fig. S13 Lifetime-associated spectra of the CS states of various hybrid rods obtained from the global-lifetime analysis.

Table S2. Fit parameters for the recovery of the XB bands at 645 nm obtained by femtosecond-resolved transient-absorption measurements.[a]

Samples	ΔA_1 (mO.D.)[b]	τ_1 (ps)	ΔA_2 (mO.D.)	τ_2 (ps)	ΔA_3 (mO.D.)	τ_3 (ps)	ΔA_4 (mO.D.)	τ_4 (ps)	ΔA_5 (mO.D.)	τ_5 (ps)
Bare rod	0.743 [±0.032][b]	0.21 [±0.01]	-0.191 [±0.006]	2.55 [±0.13]	-0.360 [±0.004]	307 [±7]	-1.32 [±0.00]	5020 [±50]		
Round	-0.305 [±0.08]	0.20 [±0.05]	-0.082 [±0.093]	0.54 [±0.30]	-0.033 [±0.002]	20.5 [±3.5]	-0.024 [±0.002]	380 [±61]	-0.069 [±0.001]	100000 [fixed][c]
Cubic	-0.497 [±0.015]	0.46 [±0.02]	-0.239 [±0.015]	2.38 [±0.23]	-0.062 [±0.007]	21.2 [±3.7]	-0.018 [±0.003]	293 [±76]	-0.030 [±0.001]	100000 [fixed]
Rough	-0.468 [±0.023]	0.28 [±0.02]	-0.184 [±0.024]	1.20 [±0.20]	-0.043 [±0.008]	9.27 [±2.25]	-0.012 [±0.002]	287 [±87]	-0.037 [±0.001]	100000 [fixed]

[a] All transients were fitted to $I(t) = \sum_i A_i \exp(-t/\tau_i)$ convoluted with the Gaussian instrument response function of 200 fs. [b] Errors in the fits.

[c] Time constants were fixed as 100 ns because of the limited time window of the measurements.

Table S3. Fit parameters for the recovery of the negative-absorption bands in **Fig. 3d**.[a]

Samples	ΔA_1 (%)	τ_1 (ns)	ΔA_2 (%)	τ_2 (ns)	ΔA_3 (%)	τ_3 (ns)	ΔA_4 (%)	τ_4 (ns)
Bare rod	50.8 [±0.8][b]	0.82 [±0.02]	29.9 [±0.6]	4.66 [±0.17]	16.2 [±0.6]	21.9 [±0.9]	3.0 [±0.2]	159 [±10]
Round	26.1 [±1.8]	6.45 [±0.90]	28.1 [±1.4]	130 [±14]	22.9 [±1.2]	2300 [±300]	22.9 [±1.1]	65000 [±7000]
Cubic	42.1 [±6.3]	3.80 [±1.02]	20.3 [±3.4]	96.6 [±35.1]	19.2 [±3.0]	2100 [±700]	18.4 [±2.7]	92000 [±40000]
Rough	21.1 [±4.6]	11.8 [±5.3]	23.4 [±4.2]	160.4 [±59.7]	27.6 [±3.8]	3400 [±1000]	27.9 [±3.9]	94000 [±34000]

[a] All transients were fitted to $I(t) = \sum_i A_i \exp(-t/\tau_i)$ convoluted with the Gaussian instrument response function of 200 ps. [b] Errors in the fits.

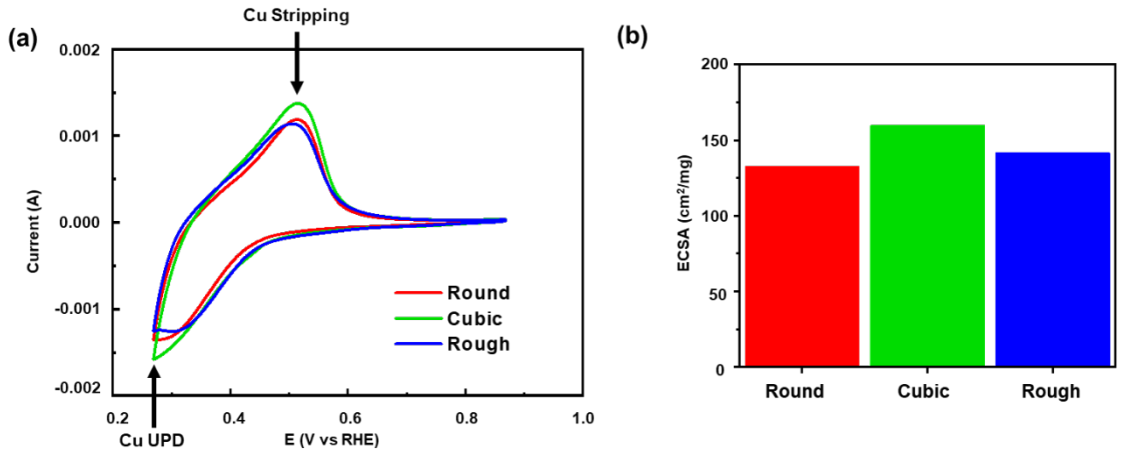

Fig. S14 (a) Cyclic voltammograms in nitrogen-saturated 0.05 M H_2SO_4 + 0.05 M $CuSO_4$ solutions at a scanning rate of 5 mV s^{-1}. (b) ECSAs estimated from (a).

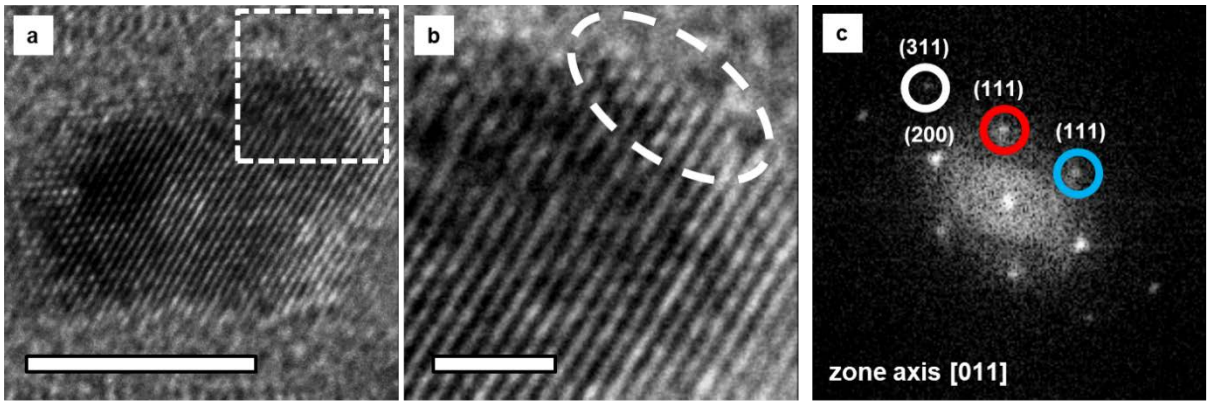

Fig. S15 (a) HRTEM image and (b) surface analysis of the (311) facet (white circle) for **Rough**. (c) Fast Fourier transform (FFT) of (b). The bars represent (a) 5 nm and (b) 1 nm.

References

S1. J. Y. Choi, W.-W. Park, B. Park, S. Sul, O.-H. Kwon and H. Song, *ACS Catal.*, 2021, **11**, 13303–13311.

S2. D. Li, C. Wang, D. Tripkovic, S. Sun, N. M. Markovic and V. R. Stamenkovic, *ACS Catal.*, 2012, **2**, 1358–1362.

S3. M. Shao, J. H. Odell, S.-I. Choi and Y. Xia, *Electrochem. commun.*, 2013, **31**, 46–48.

S4. J. Y. Choi, D. Jeong, S. J. Lee, D.-G. Kang, S. K. Kim, K. M. Nam and H. Song, *Nano Lett.*, 2017, **17**, 5688–5694.

S5. H.-W. Nho, W.-W. Park, B. Lee, S. Kim, C. Yang and O.-H. Kwon, *Phys. Chem. Chem. Phys.*, 2022, **24**, 1982–1992.

S6. K. E. Knowles, E. A. McArthur and E. A. Weiss, *ACS Nano*, 2011, **5**, 2026–2035.

S7. V. I. Klimov and D. W. McBranch, *Phys. Rev. Lett.*, 1998, **80**, 4028–4031.

S8. C. Burda, S. Link, M. Mohamed and M. El-Sayed, *J. Phys. Chem. B*, 2001, **105**, 12286–12292.

S9. M. D. Garrett, A. D. Dukes III, J. R. McBride, N. J. Smith, S. J. Pennycook and S. J. Rosenthal, *J. Phys. Chem. C*, 2008, **112**, 12736–12746.

S10. K. Wu, Q. Li, Y. Du, Z. Chen and T. Lian, *Chem. Sci.*, 2015, **6**, 1049–1054.